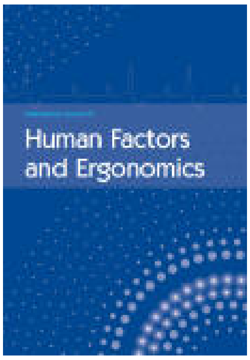

International Journal of Human Factors and Ergonomics

ISSN online: 2045-7812 - ISSN print: 2045-7804
https://www.inderscience.com/ijhfe

A case study of digital human modelling assisted occupant packaging design: comparing driving posture and position prediction methods

Estela Perez Luque, Erik Brolin, Pernilla Nurbo, Maurice Lamb, Dan Högberg

DOI: 10.1504/IJHFE.2025.10075068

Article History:

Received:	31 May 2025
Last revised:	03 October 2025
Accepted:	03 October 2025
Published online:	12 December 2025

A case study of digital human modelling assisted occupant packaging design: comparing driving posture and position prediction methods

Estela Perez Luque* and Erik Brolin

School of Engineering Science,
University of Skövde,
Skövde, Sweden
Email: estela.perez.luque@his.se
Email: perezluque.estela1504@gmail.com
Email: erik.brolin@his.se
*Corresponding author

Pernilla Nurbo

Ergonomics,
Volvo Cars,
Gothenburg, Sweden
Email: pernilla.nurbo@volvocars.com

Maurice Lamb

School of Informatics,
University of Skövde,
Skövde, Sweden
Email: maurice.lamb@his.se

Dan Högberg

School of Engineering Science,
University of Skövde,
Skövde, Sweden
Email: dan.hogberg@his.se

Abstract: Accurately predicting driving postures and positions is crucial for occupant packaging design to accommodate diverse drivers. However, this is challenging due to individual variability and limited access to user data. Digital human modelling (DHM) tools enable posture prediction in virtual environments. This paper presents a case study comparing two driving prediction methods: a statistical prediction method (SPM) and an optimisation prediction method (OPM). Both were evaluated using data from two car models with different seat heights, involving 199 participants whose seat, eye-point, and steering wheel positions were measured. Results showed SPM was more accurate for vertical positioning, whereas OPM for fore-aft positioning. The effectiveness of each method varied by car model, with SPM aligning better in the higher-seated vehicle and OPM performing better in the lower-seated vehicle. These findings highlight the practical, context-specific performance of posture prediction methods. Methodological insights guide the improvement of DHM tool use in occupant packaging.

Keywords: occupant packaging design; digital human modelling; DHM; driving posture; seated posture prediction; driver position; statistical regression; optimisation method; ergonomic simulation; H-point prediction; eye-point prediction; steering wheel position; vehicle interior design; automotive ergonomics.

Reference to this paper should be made as follows: Perez Luque, E., Brolin, E., Nurbo, P., Lamb, M. and Högberg, D. (2025) 'A case study of digital human modelling assisted occupant packaging design: comparing driving posture and position prediction methods', *Int. J. Human Factors and Ergonomics*, Vol. 12, No. 5, pp.27–57.

Biographical notes: Estela Perez Luque received her PhD from the University of Skövde. Her research interests include digital human modelling, simulation, and the prediction of human posture and motion in product and production development processes. Her work focuses on improving the usability, accuracy, and integration of human–product interaction simulations to support decision-making in early design stages.

Erik Brolin is Senior Lecturer in Product Design Engineering at the University of Skövde, where he leads the anthropometry research domain of the group User-Centred Product Design. He researches statistical body-shape modelling, anthropometric diversity and methods for virtual product and production development. His work aims to improve the accuracy and representativeness of digital human models across a wide variation of body sizes and shapes.

Pernilla Nurbo is Technical Leader for Ergonomics at Volvo Cars, where she leads the development and integration of ergonomics methods and human-centred design principles within vehicle development processes. She has extensive industrial experience in occupant packaging, digital human modelling, and ergonomic assessment, and works to ensure that human factors knowledge is effectively implemented across cross-functional automotive development teams.

Maurice Lamb is a Senior Lecturer at the University of Skövde. Maurice is an interdisciplinary researcher with a background in cognitive science, philosophy, engineering, and computer science. His primary research interests lay in applying complex dynamical systems methods to solving challenges in human-robot and human-agent interaction contexts.

Dan Högberg is a Professor at the School of Engineering Science at the University of Skövde. He focuses his research on making user-centred information, e.g., ergonomics knowledge, relevant and easily available to product designers and engineers. Central in his research is digital human modelling and how such technology can contribute to supporting designers and engineers to consider ergonomics/human factors proactively at virtual stages of the design process.

1 Introduction

Designing a vehicle interior to accommodate a wide range of drivers and passengers is the primary aim of occupant packaging design. Accurately predicting the seated posture and drivers' positions is crucial for effective occupant packaging design because it allows designers to optimise the vehicle interior for comfort, control accessibility, and visibility, among other ergonomic aspects, within the constraints of the vehicle geometry (Bubb et al., 2021). This predictive capability is particularly important as modern vehicles evolve to meet increasingly diverse user needs and expectations (Parida et al., 2020). Without accurate posture prediction, designers would have to rely on their own experience, previous designs, or extensive physical prototyping. These approaches are time-consuming, costly, and risk the accommodation of the target population (Wolf et al., 2020; Demirel et al., 2021; Perez Luque et al., 2022).

Integrating posture prediction capabilities into CAD and simulation tools in the design process provides designers with decision-support methods to develop vehicles that aim to meet ergonomic requirements. Further, to ensure inclusive, comfortable, and safe designs, human variability must be considered when predicting driver postures and key positions of their bodies, such as the H-point and eye-point. Variability can be related to differences in anthropometrics, behaviour, and individual preferences (Wolf et al., 2022; Jeong et al., 2023). For instance, shorter people typically sit more forward and higher within the seat adjustment range, while taller people usually prefer more rearward and lower positions within the seat adjustment range (Jonsson et al., 2008; Peng et al., 2018). Moreover, people with similar anthropometrics may behave and have different preferences, making them adopt substantially different driving postures (Peng et al., 2018). Consequently, driver prediction models should reflect these human differences in driving posture. Different driving posture models have been developed through data-driven and optimisation approaches. Data-driven or statistical regression models generally predict the coordinates or body joint angles of specific positions of humans in the car interior. These regression models may consider different parameters from humans, such as gender, anthropometry, age, or body symmetry, and vehicles, such as vehicle class, seat designs, or driving venues (Reed et al., 2002; Park et al., 2016a, 2016b; Wu et al., 2022). In contrast, optimisation methods predict human postures using optimisation algorithms. It is often assumed that comfort or optimal joint angles are achieved when the torques across the joints are passively balanced. Consequently, postures can be predicted by assuming that individuals select postures that allow as many joints as possible to be close to the optimal angle (Yang et al., 2005; Hanson et al., 2006; Schmidt et al., 2014; Park et al., 2015). Thus, optimisation works by minimising deviations from the optimal angles within a search space usually restricted by defined constraints, such as roof height and available seat adjustment range, to achieve a desired prediction result. This process involves three essential components: determining the set of optimal joint angles, identifying the cost functions associated with deviations from the optimal posture, and determining how these costs are traded off or optimised (Reed et al., 2000). Numerous studies have investigated what defines optimal driving postures or joint angles. However, these have mainly been used as evaluation standards for assessing posture comfort or quality, rather than as a direct prediction method (Porter and Gyi, 1998; Schmidt et al., 2014).

Vehicle designers have traditionally used two- and three-dimensional accommodation tools provided by SAE International (formerly known as the Society of Automotive Engineers) for occupant packaging design. These tools help determine the layout of recommended seat positions, head contours, eye ellipses, and hand-reach envelopes to optimise driver ergonomics. However, due to the increasing complexity of occupant packaging design, designers have supplemented these traditional tools with three-dimensional human simulation tools over the past few decades, also known as digital human modelling (DHM) tools (Scataglini and Paul, 2019). DHM tools offer a broader framework for analysing occupant packaging design, including tasks like ingress and egress, compared to SAE guidelines (Bubb et al., 2021). However, for posture prediction, SAE practices incorporate postural variability unrelated to driver or vehicle-specific variables, whereas the accuracy of DHM tools relies on the underlying assumptions of their predictive models, which can limit their accuracy and represent a general limitation in their application. An example of a DHM tool that has implemented a data-driven approach is Jack (Raschke and Cort, 2019), which uses a so-called cascade modelling approach, based on laboratory experiments with US subjects in specific vehicle package setups to predict driver positions (Reed et al., 2002). Another example of a data-driven approach implementation is a parametric CAD accommodation model for fixed heel point (FHP) driving position, which provides geometric boundaries for equipped soldiers in military vehicles (Huston et al., 2024). In addition, Brolin et al. (2020) demonstrated that statistical prediction methods (SPM) can be implemented in a DHM tool, which, at its core, has an optimisation-based prediction approach. However, developing regression models that account for all human and vehicle parameters affecting seated driving posture is challenging for a data-driven approach due to the inherent complexity and numerous variables involved in driving situations, which must be accurately captured during data collection experiments. An example of DHM tools using an optimisation approach is RAMSIS (Wirsching, 2019), with optimal angles based on a study by Seidl (1994). Limitations of the optimisation approach include that the prediction models are not as accurate as the data-driven models for specific cases (Reed et al., 2000) and do not currently include anthropometry-specific comfort joint angles (Brolin et al., 2020).

While various posture prediction models have been proposed, few studies have explored how such models perform when applied in real vehicle configurations under industrial conditions. A notable exception is Reed et al. (2000), who compared prediction methods in a lab mock-up setting. However, with the growing integration of DHM tools in automotive workflows, it remains useful to examine how existing prediction approaches behave in specific contexts. Unvalidated predictions in DHM tools may lead to design inaccuracies that compromise ergonomic quality, increase development costs due to redesign iterations, or even affect occupant safety in real-world use. Thus, improving the empirical validation of posture prediction methods is essential not only for tool reliability but also for advancing human-centred vehicle design.

This paper presents a case study conducted in an automotive industrial setting to compare two existing prediction methods, a statistical regression-based method (SPM) and an optimisation-based method (OPM), for seated driving posture. Rather than aiming to generalise to all vehicle types or populations, the objective is to examine how each method performs in relation to real-world data from two vehicles with distinct seat configurations. Through this comparison, the case study aims to provide insights into the strengths and limitations of each approach when applied in a specific design scenario.

This case-based approach contributes to understanding how DHM prediction methods function in practice and supports reflection on their selection and application in vehicle interior design.

2 Method

2.1 Data collection context

This case study was conducted in collaboration with an automotive manufacturer, using real-world data collected in two Volvo Cars vehicle models. The vehicles represent contrasting seating configurations relevant for occupant packaging design considerations: Vehicle A featured a lower seat configuration, H30 = 265 mm and L6 = 563 mm, and Vehicle B a higher seat configuration, H30 = 310 mm and L6=540 mm (all vehicle dimension definitions according to SAE J1100, 2009) (Figure 1). The chosen vehicles illustrate common seating arrangements found in regular mid-size/large cars (Vehicle A) and SUVs (Vehicle B). This difference in seat height and interior setup offers a meaningful basis for assessing how prediction methods perform under various ergonomic conditions common in the automotive industry. The test participants were given verbal instructions to adjust the seat, steering wheel, backrest angle, and mirrors until they felt comfortable, safe, and ready to drive in a driving session of 10 minutes in a real traffic situation. This was repeated three times, and the seat position and steering wheel position data were collected after the third driving session for each test participant. Before each trial, participants were asked to re-adjust the seat from an extreme, non-driving configuration (e.g., fully forward and reclined) to ensure active engagement in finding a preferred driving posture. The goal was to allow natural posture selection without imposing constraints or fixed starting points.

Figure 1 Volvo car models used in the user study (a) vehicle a and (b) vehicle b (see online version for colours)

(a) (b)

The data collection followed a procedure developed at Volvo Cars, which has been iteratively refined by the company for internal posture validation studies (Lejon and Thorsén, 2013). This approach enables repeatable seat positioning and coordinate capture of key occupant landmarks using in-vehicle sensors and external measurement tools. Although the data collection was conducted for each vehicle separately, the same measurement procedure, participant instructions, and posture capture methods were used across both vehicles to ensure consistency.

To determine the H-point, the vehicle's built-in seat motors were used to capture each participant's final seat configuration, including longitudinal position, seat height, and backrest recline angle. These motor values were stored by the seat control unit and corresponded to predefined non-nominal positions in the vehicle interior geometry. Each recorded seat configuration was mapped to its corresponding H-point using internal lookup tables based on Volvo's design reference data. This approach allowed precise retrieval of the H-point in 3D space without the need for manual measurement. The resulting H-point coordinates were then transformed to the vehicle's package coordinate system, which used the seating reference point (SgRP) as origin and followed SAE J1100 definitions.

To determine the eye-point, a side-view camera was mounted inside the vehicle, aligned with the driver's sagittal plane. A photograph was taken while the participant was driving straight during the third session. The camera setup was calibrated using a checkered reference grid to correct for lens distortion. In the image, the approximate centre point between the participant's eyes was manually selected. This pixel location was then translated into a 3D coordinate in the vehicle's reference system using the known camera geometry and seat configuration. Only images with clear visibility of both eyes and minimal head rotation were used in the analysis.

The position of the steering wheel centre was obtained from a separate photograph taken from above the steering wheel. As with the eye-point photo, the image was corrected using a reference grid to ensure geometric accuracy. The centre of the steering wheel, typically corresponding to the horn button, was manually marked in the image and then projected into the vehicle coordinate system using the same calibration and transformation principles. This process replaced earlier manual measurement methods and improved the consistency of steering wheel location data across vehicles. Internal validation tests confirmed that the H-point and eye-point positions could be measured with a repeatability of approximately ±10 mm and ±5 mm, respectively (Lejon and Thorsén, 2013).

Test participants were recruited from Volvo Cars staff, and they were not involved in the study's planning, design, or execution. In total, 104 participants were involved in collecting data for Vehicle A (study conducted in 2017), and 95 participants were involved in collecting data for Vehicle B (study conducted in 2018). The anthropometric data of the participants is described in Table 1.

Participants were selected to reflect a broad range of body measurements rather than to represent a population sample, with emphasis on including both shorter and taller individuals. As the collective anthropometric diversity of the participants did not follow a normal distribution, they were divided into three groups based on height: short (1,460–1,634 mm), medium (1,635–1,795 mm), and tall (1,796–2,030 mm). Each group comprised approximately 1/3 of the total number of participants, ensuring a balanced representation of different statures. No separation was made between male and female participants regarding height distribution, as the analysis focused on stature regardless of gender.

Table 1 Summary of anthropometric data of participants involved in the case study

		Vehicle A				*Vehicle B*			
Gender		*Females*		*Males*		*Females*		*Males*	
Subjects		*44*		*60*		*39*		*56*	
Anthropometric measurements		*Mean*	*SD*	*Min*	*Max*	*Mean*	*SD*	*Min*	*Max*
1	Stature without shoes	1,730	128	1,460	1,981	1,735	150	1,460	2,030
2	Weight (kg)	72	17	44	148.5	74	20	44	138.5
3	Waist circ., standing	857	110	665	1260	868	127	630	1270
4	Hip width, standing	351	23	300	424	353	27	300	422
5	Upper arm length	353	31	300	428	355	39	295	454
6	Elbow-fingertip	455	40	374	550	456	45	365	560
7	Sitting height	920	58	802	1,045	920	66	802	1,106
8	Hip width, sitting	383	26	334	478	385	31	335	481
9	Buttock to front of knee	601	51	496	756	606	59	496	756
10	Buttock to back of knee	486	43	407	615	489	50	405	615
11	Knee height sitting, without shoes	531	53	439	667	538	60	440	699
12	Foot width without shoes (left)	94	9	74	113	95	9	74	114
13	Foot length without shoes (left)	249	22	206	304	250	26	189	312

Note: In millimetres (mm) unless otherwise noted.

2.2 Statistical prediction method

The driver posturing process involves several parameters where both the steering wheel and seat can move independently of each other. In which order this process is done might vary between vehicles and drivers, i.e., it is not certain that the steering wheel position is set before the seat is positioned or vice versa. The positioning of the steering wheel and seat is rather done iteratively, more or less in relation to each other. In the study of this paper, the intention is to predict the position of all adjustable parts of the driver interior within given constraints, such as adjustment ranges of the steering wheel and seat. To implement a SPM that includes both prediction of steering wheel position and seat position, a specific sequence of these predictions needs to be decided. The SPM uses two different prediction models in a sequence of three steps:

1 first, a prediction of the fore-aft steering wheel position is done (Reed, 2013)

2 followed by a prediction of the H-point position (Park et al., 2016b)

3 to eventually be able to predict the position for the centre-eye point (Park et al., 2016b).

The fore-aft steering wheel position (L6) is a dimension that is set for each vehicle (SAE J3099, 2024). The steering wheel can usually move within an adjustment range, where L6 is defined at the centre of this range. The prediction of the steering wheel location is made by using a model that was initially developed as an ordinal logistic regression to predict the distribution of subjective responses as a function of fore-aft steering wheel position (L6), seat height (H30), and driver stature (Reed, 2013). In the study, subjective responses were measured on a rating scale that varied from 1 to 7. Response 4 was counted as 'just right' and in this study inserted into a transformed linear part of the logistic model to be able to predict a preferred fore-aft steering wheel location (L6) (mm) as

$$L6 = 4 + 0.003441 \times Stature + 0.01854 \times H30 - 0.0004958 \times H30^2 0.02282 \tag{1}$$

Table 2 Driver posture-prediction models for the cascade modelling approach (Park et al., 2016b).

Female driver posture-prediction		
Dependent variable	*Regression model (mm)*	*RMSE (mm)*
H-point x re PRP	678 + 0.284 × S–494 × SHS + 2.33 × BMI–0.388 × H30 + 0.426 × (L6-600)	24.9
H-point z re AHP	129-6.2 × 10^{-2} × S + 0.909 × H30–4.65 × 10^{-2} × (L6-600)	12.4
Centre-eye x re H-point	–364 + 7.64 × 10^{-2} × S + 540 × SHS + 0.124 × (L6-600)	37.7
Centre-eye z re H-point	–461 + 0.163 × S + 1445 × SHS-15.1 × BMI + 3.61 × age + 9.93 × 10^{-3} × S × BMI-6.54 × SHS × age	12.7
Male driver posture-prediction		
Dependent variable	*Regression model (mm)*	*RMSE (mm)*
H-point x re PRP	–48 + 0.56 × S + 1.39 × BMI + 7.53 × age–0.42 × H + 0.505 × (L6-600)–3.98 × 10^{-3} × S × age	25.3
H-point z re AHP	123.1–5.864 × 10^{-2} × S + 0.945 × H30	10.6
Centre-eye x re H-point	–578 + 0.174 × S + 706 × SHS–1.55 × BMI-6.48 × 10^{-2} × H30	32.1
Centre-eye z re H-point	–498 + 0.361 × Stature + 845 × SHS + 2.76 × BMI-0.175 × age	14.4

Notes: S = stature (mm); SHS = sitting height/stature; BMI = body mass index (kg/m^2); H30 = seat height (mm).

If the predicted preferred fore-aft steering wheel location (L6) is outside the adjustment range, then the location is moved to the closest point of the adjustment range area. The predicted preferred fore-aft steering wheel location is subsequently used as the L6 value, instead of the actual L6 value of the vehicle, to predict coordinates for the preferred seat position, i.e., the H-point, with an x-coordinate in relation to the ball of foot point (BOF) and a z-coordinate in relation to the accelerator heel point (AHP). In the study by Park et al. (2016b), the L6 value was set in different predefined positions, and participants were not allowed to change it. As a result, the prediction models could use different L6 values as predictive variables, where the recommendation is to use the vehicle L6 value in the centre of the steering wheel adjustment range. The motivation for using a predicted steering wheel location instead of the actual vehicle L6 is to statistically determine the L6 position when no predefined value is available, as well as to capture the variability found in real data, thereby reflecting a wider range of outcomes in subsequent predictions. In the third step, coordinates for the centre-eye position are predicted in relation to the H-point position. Following the method by Park et al. (2016b), different posture prediction models for men and women were used (Table 2). Table 3 presents a pseudocode summary of the SPM, outlining the sequence of predictions and inputs required to reproduce the procedure.

Table 3 Pseudocode describing the implementation of the SPM, following a cascade modelling approach

	Pseudocode for SPM
1	Predict preferred fore-aft position of the steering wheel (L6):
	Use a statistical model based on driver stature and seat height [equation (1)]
	Ensure the predicted value falls within the vehicle's steering wheel adjustment range
	If it falls outside the range, adjust to the closest boundary
2	Predict seat H-point position:
	Use the predicted steering wheel position (L6) along with participant anthropometrics
	Apply gender-specific statistical models to estimate the horizontal and vertical H-point coordinates relative to vehicle reference points (Table 2)
3	Predict eye-point position:
	Use the predicted H-point along with participant anthropometric characteristics
	Apply gender-specific models to estimate the eye-point coordinates relative to the H-point (Table 2)
Output:	
	Fore-aft steering wheel position (L6)
	Predicted seat H-point (X, Z)
	Predicted eye-point (X, Z)

2.3 Optimisation prediction method

The second method for predicting driving postures involves an optimisation approach. In this study, the version 2023-R2-SP2 of the DHM tool IPS IMMA was used to represent the optimisation prediction method (OPM) for occupant packaging design (Hanson et al., 2019). IPS IMMA is a commercially available DHM software developed for industrial applications. It is used in both academic research and commercial settings, particularly in the automotive sector, for ergonomics analysis and human-centric design (IPS IMMA, 2025). The optimisation model employed in the software is based on the principles described by Bohlin et al. (2012) and Delfs et al. (2013). This model predicts the driver's posture by solving an optimisation problem that seeks to maximise a comfort function, which evaluates ergonomic factors such as joint angles, joint torques, and proximity to obstacles. The optimisation is expressed as:

$$maximize\ h(x) \quad while: g(x) = 0$$

where $h(x)$ represents the comfort function, prioritising postures that minimise joint strain and maintain ergonomic alignment, and $g(x)$ refers to kinematic constraints such as body segment alignments (positioning constraints) and biomechanical balance. The driver's optimal joint angles, which are the basis of the optimisation in the software, were originally derived from a study by Bergman et al. (2015) and adjusted to fit the biomechanical model of IPS IMMA. In addition, collision avoidance is also included by penalising postures where body parts approach environmental obstacles. The iterative optimisation process refines the posture prediction until it satisfies all the constraints while maximising the comfort function.

The DHM scene consisted of a group of manikins and the geometries of each of the two vehicle types. The manikin family corresponding to each vehicle represents the drivers who participated in the data collection, i.e., manikins were created with the same anthropometric measurements as the participants (Table 1). A standard DHM simulation setup was followed to make manikins adopt an initial seated driving posture (Perez Luque et al., 2022).

First, several basic constraints were established to ensure that the manikins could perform the necessary driving tasks. These basic constraints included positioning the feet on the pedals, placing the hands on the steering wheel, ensuring that the hip joint falls within the H-point envelope, and aligning the torso with the mid-back seat using attachment points in the DHM tool (Figure 2). For the foot positioning, the right BOF was placed on the accelerator pedal and the left BOF in a resting position, with both AHPs in contact with the vehicle floor. These constraints were implemented using attachment points, which restrict the manikins to only move within a defined two or three-dimensional range (such as a line, a plane, or a box), as illustrated in Figure 2 (Hanson et al., 2019).

Furthermore, four additional constraints were introduced to better simulate how participants were instructed to select a comfortable and safe driving posture during the data collection. These constraints aimed to reflect realistic spatial limitations and visual requirements typically considered by drivers. Three of the additional constraints focused on avoiding collisions with surrounding vehicle geometries, specifically, ensuring sufficient clearance between the head and the roof, the knees and interior surfaces, and the thighs and the steering wheel. These were implemented using the DHM tool's collision avoidance functionality (Figure 2). The fourth constraint was defined to ensure a minimum height of the eye-point above the steering wheel, reflecting the driver's need to see over the steering wheel and the front (hood) of the vehicle. This constraint was inspired by the concept of the downward vision angle illustrated in Parkinson's work on occupant packaging, where the angle is defined from the eye-point to the hood surface (Parkinson and Reed, 2006). However, in this study, the reference was adapted to extend from the hood to the top of the steering wheel (in its lowest adjustment position), ensuring that the eye-point of the manikin remained above this level (down vision angle in Figure 2). This was implemented using the attachment point functionality. While not all drivers may follow these additional constraints, they were developed in collaboration with Volvo ergonomics experts to reflect common assumptions about typical driver behaviour. Together, these additional constraints helped ensure that predicted postures also approximated the comfort and safety considerations expected in real drivers.

Finally, the ‘driving car’ strategy in the DHM tool was used to generate the posture prediction using the OPM. This strategy consists of a predefined set of specific joint angles typical for a driving posture obtained in a previous research study (Bergman et al., 2015). The software then calculates the optimal posture that minimises deviation from this set of specific joint angles while fulfilling the basic and additional constraints.

An overview of the step-by-step procedure followed to implement the OPM in the DHM tool is presented in Table 4 as pseudocode. Additionally, the Lua scripts used to define and implement the basic constraints in IPS IMMA as well as generating the final output in the form of coordinates of H-point, eye-point, and steering wheel position are available via a GitHub repository (Brolin, 2025).

Figure 2 DHM tool scene setup for posture prediction in the case study (see online version for colours)

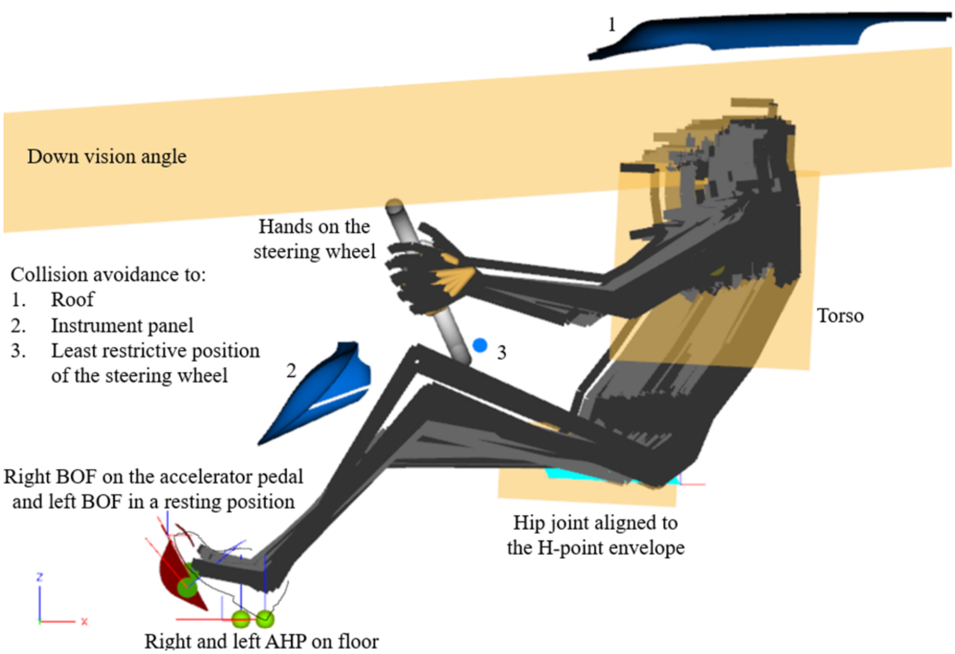

Notes: Manikins seated with basic and additional constraints. Basic constraints ensured necessary driving tasks functionalities (e.g., both heels on the floor with the right foot on the pedal, hands on the steering wheel), while additional automotive-specific constraints improved realism (e.g., collision avoidance and a minimum height for vision).

Table 4 Pseudocode outlining the procedure for posture prediction using the OPM in IPS IMMA

	Pseudocode for OPM
1	Initialise DHM scene:
	Load vehicle geometry (Vehicle A or B)
	Create manikins using participant-specific anthropometric data (Table 1)
2	Define basic posture constraints for the driving task by attachment points:
	Feet on pedals and floor
	Hands on steering wheel
	Hip joint within H-point envelope
	Torso aligned with mid-back seat using attachment points
3	Define additional constraints for replicating a comfortable and safe posture:
	Collision avoidance to geometries around (head, knees, thighs)
	Downward vision angle (attachment point) to ensure Eye-point height above steering wheel
4	Set the 'driving car' strategy (IPS IMMA predefined set of joint angles)
5	Solve optimisation problem:
	Maximise comfort function $h(x)$ and minimise deviation from default 'driving car' joint angles
	While satisfying constraints $g(x) = 0$
Output:	
	Optimal posture prediction for each manikin satisfying all constraints together with coordinates of H-point, eye-point, and steering wheel position

3 Results

This section outlines the driving positions obtained for each manikin group in vehicles A and B using the two prediction methods, compared to the real-world collected data. The results show the location of driver key variables: the H-point, eye-point, and steering wheel position.

3.1 H-point prediction

Figure 3 illustrates the predicted H-point using SPM (blue points) and OPM (orange points) against the real collected data (black points) for Vehicle A and Vehicle B. Figure 3 also shows results when residual variance (RV), i.e., a degree of randomness, is included in the SPM using the RMSE values given by Park et al. (2016b) together with a stochastic component from a standard normal distribution. Additionally, Figure 3 also illustrates results for the OPM when loosening constraints (LC) are applied, specifically a doubled range of the hip joint attachment in the Z direction.

Table 5 Comparison of prediction methods for H-point

		Average error (SD)		*Correlation*		*MAE*		*RMSE*	
		Vehicle A	*Vehicle B*	*Vehicle A*	*Vehicle B*	*Vehicle A*	*Vehicle B*	*Vehicle A*	*Vehicle B*
H-point x (mm)	SPM	–28.4 (40)	–50.3 (33)	0.8	0.9	39.7	53	48.8	59.9
	OPM	27.2 (75)	31.9 (37)	0.9	0.9	38.3	38.4	47.2	48.5
	SPM (RV)	–27.2 (45)	–51.5 (38)	0.8	0.9	42.3	55.8	52.3	63.7
	OPM (LC)	27.2 (39)	31.9 (37)	0.9	0.9	38.3	38.4	47.2	48.5
H-point z (mm)	SPM	–2.1 (23)	6.3 (21)	0.7	0.8	20.4	19.7	23.4	22.3
	OPM	6.7 (26)	9.4 (25)	0.4	0.4	22.6	22.6	26	26.2
	SPM (RV)	–5.1 (24)	4.9 (24)	0.4	0.4	20.9	20.5	24.8	24.5
	OPM (LC)	4.7 (24)	7.1 (24)	0.4	0.4	20.8	21.1	24.8	25.4

Notes: average error (mean of the predicted minus measured) and Standard deviation (SD) of the average errors; Pearson correlation; mean absolute error (MAE); and root mean squared error (RMSE) between observed and predicted data.

Figure 3 Comparison of h-point prediction by SPM (blue points) and OPM (orange points), including both standard (filled) and extended versions (open circles for RV and LC, respectively), against real collected data (black points) for (a) Vehicle a and (b) Vehicle b (see online version for colours)

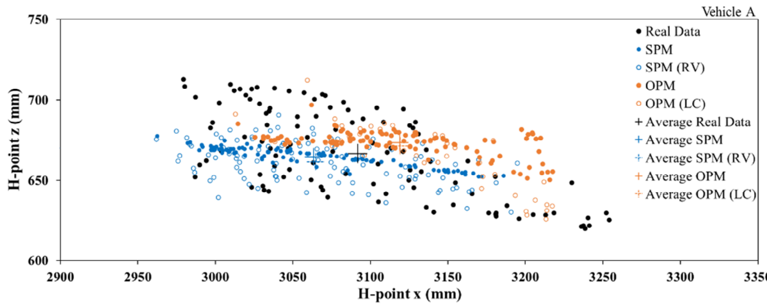

(a)

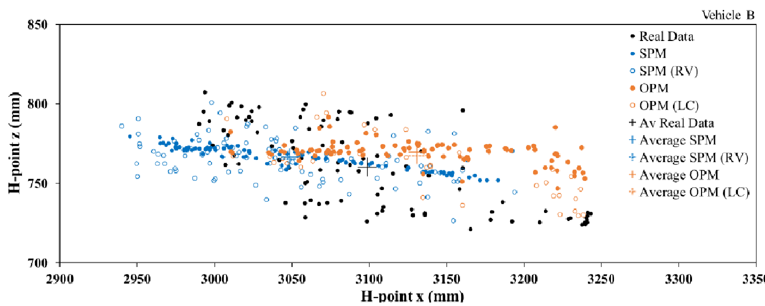

Note: Cross markers represent group averages.

3.1.1 Vehicle A

In the x-axis (fore-aft direction), there is a noticeable trend where OPM predicts the H-point further back, while SPM predictions tend to be more forward (Figure 3). In this way, OPM predictions could be unable to accurately predict more forward positions, whereas SPM could be failing to cover some of the people who sit further back within the H-point envelope. This tendency of forward prediction by SPM and rearward prediction by OPM is consistent across most data points for Vehicle A, indicating a potential tendency of these methods to position the driver slightly further forward (SPM) or back (OPM) than the real-world measurements. In the z-axis (vertical direction), OPM tends to predict a higher H-point than SPM (Figure 3). SPM's z-axis predictions exhibit a narrower spread in the z-direction, whereas OPM captures a wider range of z-axis positions (Figure 3). However, this increased variability does not necessarily correlate with the actual measurements, indicating a potential overestimation in vertical positioning. This suggests that both methods struggle to accurately capture the variability in vertical seating positions, with OPM overestimating the vertical spread and SPM not fully representing the vertical spread.

Table 5 further details these observations with statistical measures. The average error for the x-axis prediction shows that SPM has a negative bias (–28.4 mm), indicating it generally predicts positions slightly forward compared to the real data. OPM, on the other hand, has a positive bias (27.2 mm), confirming its tendency to predict positions further back. The correlation coefficients for both methods are high (0.8 and 0.9), indicating a strong linear relationship with the actual data. However, the mean absolute error (MAE) and root mean squared error (RMSE) show that OPM has slightly better accuracy in the x-axis predictions. For the z-axis, SPM exhibits a lower average error (–2.1 mm), indicating it predicts better the vertical H-point position. OPM shows a slight positive bias (6.7 mm), suggesting that it predicts the H-point slightly higher on average than it actually is. The correlation for SPM is higher (0.7) than for OPM (0.4), indicating better predictive reliability in the vertical dimension. This is verified with both MAE and RMSE values, showing more pronounced errors in OPM predictions.

3.1.2 Vehicle B

For Vehicle B, similar patterns are observed as in Vehicle A, with SPM predicting the H-point further forward and OPM predicting it further back and higher in the z-axis (Figure 3). However, in Vehicle B, the errors are larger for both methods and directions, particularly for SPM in the x-axis predictions, showing a more pronounced forward prediction (–50.3 mm) (Figure 3).

3.2 Eye-point prediction

Figure 4 and Table 6 compare the predicted eye-point positions using SPM and OPM against the collected data for Vehicles A and B, respectively.

3.2.1 Vehicle A

SPM predicts a more forward eye-point position compared to the real data, with an average error of –60.3 mm, while on the other hand, OPM predicts a more rearward position with a lower average error of 13 mm (Figure 4, Table 6). However, neither method fully captures the spread of the real data in the x-axis, indicating limitations in both predictive models. The correlation for both methods in the x-axis is 0.7, showing a moderate linear relationship with the actual data. In addition, OPM shows lower error values in predicting the eye point in the x-axis than SPM.

In contrast, the z-axis predictions are relatively similar in performance, although OPM shows slightly lower error values, suggesting a marginally better fit to the real data.

3.2.2 Vehicle B

SPM predicts a more forward position, with an average error of –62.7 mm, while OPM predicts a much more rearward position with a significant error of 107.4 mm, indicating a poor fit for Vehicle B (Figure 4, Table 6).

On the z-axis, SPM achieves a low average error of –1.9 mm, closely matching the real data, while OPM shows a slight overestimation at 6.5 mm. The correlation for SPM and OPM on the z-axis is equal (0.8). However, SPM reflects better predictive accuracy in the vertical dimension observing lower error values.

Table 6 Comparison of prediction methods for eye-point

		Average error (SD)		*Correlation*		*MAE*		*RMSE*	
		Vehicle A	*Vehicle B*	*Vehicle A*	*Vehicle B*	*Vehicle A*	*Vehicle B*	*Vehicle A*	*Vehicle B*
Eye-point x (mm)	SPM	–60.3 (52)	–62.7 (63)	0.7	0.7	67.8	74.4	79.1	88.9
	OPM	13.0 (72)	107.4 (60)	0.7	0.7	39.9	110	52.3	122.8
	SPM (RV)	–57.4 (61)	–56.2 (74)	0.6	0.6	69	74.4	83.4	92.5
	OPM (LC)	14.3 (51)	107.8 (60)	0.7	0.7	40.2	110.3	52.3	123.2
Eye-point z (mm)	SPM	–10.7 (28)	–1.9 (24)	0.7	0.8	24.5	18.3	29.7	23.8
	OPM	–10.0 (38)	6.5 (26)	0.6	0.8	22.5	19.7	28.5	26.4
	SPM (RV)	–14.3 (32)	–4.6 (27)	0.6	0.8	28.5	21.8	34.8	27.7
	OPM (LC)	–12.0 (29)	4.4 (27)	0.5	0.7	24	19.9	31.2	27.3

Notes: Average error (mean of the predicted minus measured) and standard deviation (SD) of the average errors; Pearson correlation; mean absolute error (MAE); and root mean squared error (RMSE) between observed and predicted data.

Figure 4 Comparison of eye-point prediction by SPM (blue points) and OPM (orange points), including both standard (filled) and extended versions (open circles for RV and LC, respectively), against real collected data (black points) for (a) Vehicle A and (b) Vehicle B (see online version for colours)

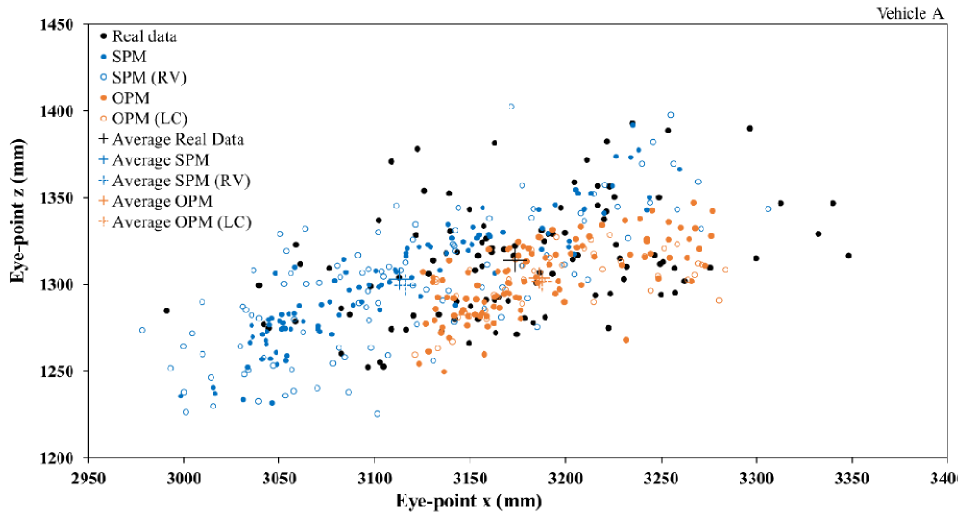

(a)

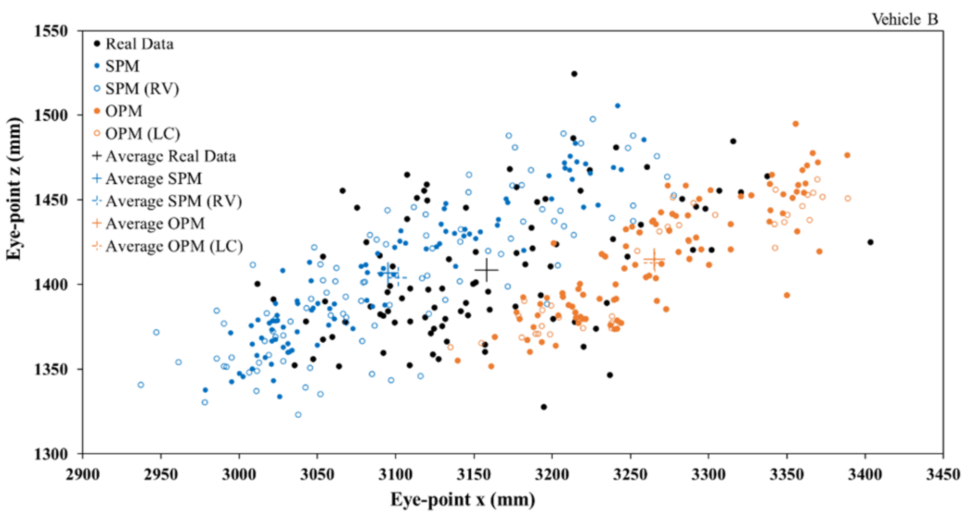

(b)

Note: Cross markers represent group averages.

3.3 Steering wheel position prediction

Table 7 shows the steering wheel position predictions in the x-axis for both Vehicle A and Vehicle B using SPM and OPM, respectively.

3.3.1 Vehicle A

For Vehicle A, OPM closely aligns with the real data, showing an average error of 4.7 mm, while SPM has a more pronounced forward bias with an average error of –18.1 mm (Table 7). OPM demonstrates slightly better predictive accuracy, with a higher correlation (0.6) compared to SPM (0.5) and lower error values for both MAE (15.2 mm) and RMSE (18.1 mm), indicating a better overall fit.

3.3.2 Vehicle B

For Vehicle B, OPM slightly outperforms SPM, with an average error of 8.3 mm compared to SPM's –10.2 mm (Table 7). The correlation for both methods is lower in Vehicle B, with OPM achieving 0.4 and SPM only 0.1, reflecting greater variability in predictive accuracy. OPM also shows lower MAE (18.4 mm) and RMSE (22 mm) than SPM.

Table 7 Comparison of prediction methods for steering wheel position

		Average error (SD)		*Correlation*	
		Vehicle A	*Vehicle B*	*Vehicle A*	*Vehicle B*
Steering wheel position x (mm)	SPM	–18.1 (18)	–10.2 (26)	0.5	0.1
	OPM	4.7 (18)	8.3 (20)	0.6	0.4
		MAE		*RMSE*	
		Vehicle A	*Vehicle B*	*Vehicle A*	*Vehicle B*
Steering wheel position x (mm)	SPM	20.5	22	25.8	27.8
	OPM	15.2	18.4	18.1	22

Notes: Average error (mean of the predicted minus measured) and standard deviation (SD) of the average errors; correlation; mean absolute error (MAE); and root mean squared error (RMSE) between observed and predicted data.

3.4 Results summary

The comparison of SPM and OPM revealed that each method demonstrates strengths depending on the specific vehicle configuration and prediction point. Table 8 summarises the best-performing method in this case study based on all evaluation metrics across both vehicles, highlighting that each method shows better alignment depending on the specific vehicle configuration. While Table 8 presents an overview of the methods' performance, additional insights are available through Bland-Altman plots, which are included in the Appendix providing a more detailed analysis. These plots visually represent the differences between predicted and measured values, helping to identify key trade-offs between precision and adaptability for each method. Boxplots of the Euclidean distances for SPM and OPM predictions are also included in the Appendix, offering a complementary visualisation of the methods' overall prediction accuracy.

Table 8 Best performing prediction method for Vehicle A and Vehicle B

	Vehicle A	*Vehicle B*
H-point x	OPM	OPM
H-point z	SPM	SPM
Eye-point x	OPM	SPM
Eye-point z	OPM	SPM
Steering wheel x	OPM	OPM

4 Discussion

This case study compares two different methods, SPM and OPM, for predicting seated driving postures and positions within vehicle occupant packaging design. SPM relies on human anthropometrics to predict the location of driver key variables such as the H-point, eye-point, and steering wheel position through a cascade modelling approach, where predictions are made sequentially. However, its base on fixed equations limits adaptability to additional constraints or variations outside the predefined parameters. In contrast, OPM assumes individuals select postures that align their joints as closely as possible to optimal joint angles, maximising their comfort. This approach is able to adapt to the constraints defined within the DHM scene. However, OPM prediction models may require refinement to represent postural variability across targeted populations better. As this study focuses on one specific implementation of SPM and OPM within the IPS IMMA tool and two contrasting vehicle configurations, the insights should be interpreted within this defined scope.

4.1 Results

The comparison between SPM and OPM for Vehicles A and B reveals differences in how each method performs across the key predicted points: H-point, eye-point, and steering wheel position.

4.1 H-point prediction

For the x-coordinate of the H-point, OPM shows better accuracy in the tested scenarios for both vehicles, outperforming SPM. Within the scope of this case, this suggests that OPM is more effective in predicting the fore-aft positioning of the occupant’s hip joint for both the low (Vehicle A) and high (Vehicle B) seat configurations. Additionally, the Bland-Altman plots reveal additional insights. For Vehicle A, SPM demonstrates narrower limits of agreement (LOA), indicating better precision, despite having a slight underprediction bias. In contrast, OPM shows wider LOA and more random scatter, which reflects greater adaptability to diverse driver postures but lower precision. A similar trend is observed in Vehicle B, where SPM maintains higher precision but exhibits a stronger underprediction bias, while OPM performs with less systematic bias but greater variability. When considering the z-coordinate (vertical positioning), SPM performs better across both vehicles, which corresponds with the Bland-Altman analysis.

This variation in performance between axes highlights the need for further development or complementary consideration of the two methods for H-point predictions.

To further investigate the poor performance of OPM in the z-axis for H-point prediction, the population was divided into three stature groups: short, medium, and tall. This was conducted to determine whether errors increase for specific stature groups, given that stature is a key aspect influencing where individuals sit within the H-point envelope (Wolf et al., 2022). Figure 5 shows that the difference error between the measured and predicted increases significantly for OPM as stature increases across both Vehicle A and Vehicle B. While OPM can more accurately predict H-point vertical positions for average-sized occupants, its predictive capability diminishes for individuals at the extremes of the stature range, especially taller drivers. SPM displays similar trends with less pronounced errors, resulting in a more consistent error distribution across all stature groups, making it a more reliable method for predicting H-point z-coordinates in vehicles where accommodating a wide range of driver statures is essential.

Figure 5 H-point z: difference errors trend line across stature (see online version for colours)

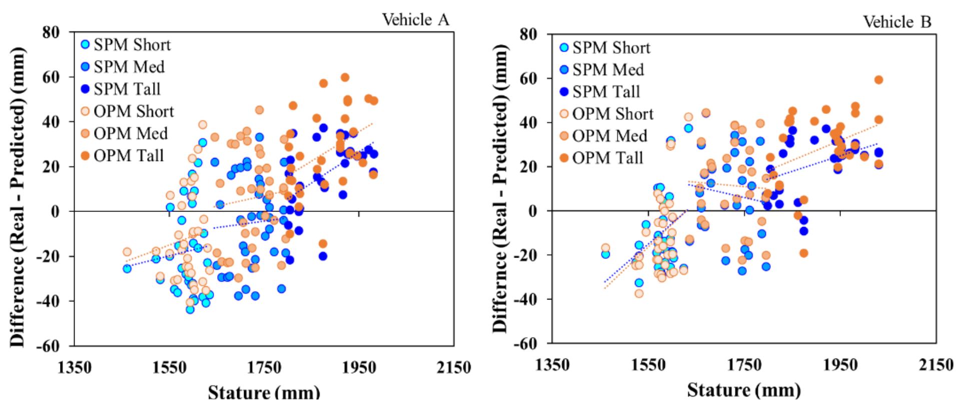

4.2 Eye-point prediction

The eye-point prediction results follow another pattern. For Vehicle A, OPM outperforms SPM in both the x- and z-axes. This suggests that OPM is more reliable in predicting eye-point locations for specific vehicle configurations similar to Vehicle A. For Vehicle B, which has a different vehicle configuration with a higher seat height, SPM performs better in both axes. This shift in prediction accuracy suggests that SPM potentially captures better the driver's seating posture and eye-point positioning in vehicle configurations similar to Vehicle B. However, the Bland-Altman plots provide additional context, showing that while OPM performs better according to metrics for Vehicle A, SPM demonstrates narrower LOA and greater precision for both x-and z-coordinates. For Vehicle B, SPM outperforms OPM across all analyses, including Bland-Altman.

4.3 Steering wheel position prediction

For the steering wheel x-coordinate, OPM again provides higher accuracy in Vehicle A and Vehicle B, indicating its potential ability to adapt to posture and steering wheel positioning requirements of vehicles with lower and higher seat heights, respectively.

4.4 Prediction method by vehicle type

Overall, considering the evaluation metrics, OPM showed better alignment with measured data for Vehicle A, which features a lower seat height in the tested scenarios. Its performance in predicting the H-point, eye-point, and steering wheel position in the x-axis suggests that the current underlying set of optimal angles used in OPM suits better the specific ergonomic configuration of lower-seated vehicles like Vehicle A. Nonetheless, the Bland-Altman analysis highlights that SPM's narrower LOA could result in better precision, even in cases where systematic bias is greater. For Vehicle B, which has a higher seat height, SPM outperforms OPM across most prediction points, particularly in the vertical (z-axis) predictions, although it does not necessarily predict the variability in it. This could indicate that the default set of optimal angles in OPM does not account for the variations in drivers' posture resulting from different vehicle configurations like Vehicle B. Consequently, a different set of optimal angles tailored for higher seat configuration vehicles could improve OPM's prediction performance. Such adjustments could potentially bring OPM's results in Vehicle B closer to the accuracy it achieves in Vehicle A with a lower seat position, suggesting its potential prediction utility across different vehicle types. Still, these findings should be interpreted in light of the studied vehicle configurations, and care should be taken not to generalise the results beyond similar contexts or tool implementations.

4.5 Limitations

While the study provides valuable insights, several limitations must be acknowledged. These relate to the number of vehicles analysed, data collection protocols, and the methods and tools evaluated. First, the study was conducted using two vehicle configurations, which represent contrasting but limited configurations. Given that this is a case study, the results should be interpreted within these specific contexts, and the generalisability of the findings to other vehicle types is limited. Future studies should incorporate a broader range of vehicle configurations to evaluate the methods more comprehensively and enable the generalisability of the results. Additionally, differences in how companies collect or estimate real-world posture data, such as alternatives in posture estimation methods or motion capture technologies, may influence the observed outcomes and their alignment with predictive models. Such methodological variation could result in different patterns and should be taken into account when comparing across industrial contexts.

Second, potential biases may have arisen from the initial seat placement during data collection, as this could have influenced how participants adjusted and selected their seating positions. Although a neutral starting position was adopted based on standard methods from previous research, a recent study has shown that starting conditions can introduce biases (Jung and Park, 2023). However, it is important to note that the methodology for collecting posture data was based on an established methodology used by the company conducting the data collection, where consistency and comparability of results are prioritised, and direct measurement in real vehicles is a key component. Future studies should consider methodologies that reduce these effects to address this, such as conducting multiple trials with varied initial seat positions.

Third, the statistical regression models from Park et al. (2016) used in this study (SPM) were originally developed based on a US population. In this study these models were applied to a non-US sample. Nevertheless, the values of the participants in this study fell within the ranges reported in the original dataset, which supports the applicability of these regression models. Future studies could further investigate how prediction accuracy is influenced by population-specific anthropometric distributions.

Additionally, the OPM used in this study incorporates additional constraints that aim to better replicate the conditions under which participants selected their driving posture, specifically, prioritising comfort and safety as instructed during data collection. One of these constraints involves a minimum eye-point height above the steering wheel. While this constraint aligns with practical design goals, its empirical basis remains limited. Previous studies have found that variations in downward visibility may not consistently influence driver posture (e.g., SAE J941, 2010), suggesting that such constraints should be interpreted with caution. Nevertheless, the use and definition of this constraint were developed in collaboration with ergonomics experts at Volvo, who consider it a reasonable reflection of common driver behaviour and expectations regarding forward visibility. Therefore, although the constraint supports the simulation of realistic posture behaviour in this specific context, its generalisability to other environments or user groups is uncertain. Future research is needed to validate whether and how visual access influences seated posture selection in diverse vehicle settings.

Lastly, this study was limited to evaluating OPM implemented in a single DHM tool, IPS IMMA. Expanding the analysis to include OPM implemented in other DHM tools could provide a broader understanding of the method's effectiveness and applicability across different DHM tools. Additionally, limitations in the specific IPS IMMA version used, such as the body models and their meshes, could have affected the accuracy of the predictions as they may not realistically represent humans. Enhancing the fidelity of these body models could lead to more accurate and reliable results, particularly in capturing the detailed postural variations of different body sizes.

4.6 Future research directions for posture prediction methods

While both methods show potential for predicting driver posture in occupant packaging design, their performance varies depending on the specific vehicle configuration. Both methods leave room for improvement, emphasising the importance of further refinement and validation of predictive models to improve their reliability and applicability. On the one hand, an advantage of SPM is that the prediction of characteristic driving positions is written as closed-form, linear equations (Table 2), which makes them independent of any human model and easier to use. In contrast, OPM must be implemented using a particular kinematic linkage or digital human model. On the other hand, one potential advantage of OPM is that it may provide more generalisable results to new design tasks as its results are a consequence of the digital human model and constraints defined in the virtual environment, whereas SPM is not able to adapt to additional constraints or aspects to the ones considered in their equations. Furthermore, analysing a specific vehicle configuration can be crucial when choosing prediction methods. This study shows that the set of optimal joint angles for OPM used in this study may yield better prediction results for vehicles with lower seat configurations, while SPM shows better performance for vehicles with higher seat configurations.

While both SPM and OPM present distinct advantages depending on the application, there remain areas where each method could be refined to better capture the complexity of human posture across different vehicle configurations. SPM could be enhanced by adjusting the results using the average error found compared to real world data. Based on the average error of this initial evaluation, adjustments could be made following the same sequence as the cascade modelling approach. Thus, the average error for the steering wheel position would be calculated first, and the adjustment of those predictions would be added before the average error of the H-point position could be calculated next. Lastly, the average error of the centre-eye position could be calculated after adjustments to predictions of the H-point have been added. Different adjustments could be calculated for different vehicle models.

As observed in Figure 5, OPM's error performance particularly increases depending on the stature, suggesting that the optimal angles used in the optimisation process could be further refined for specific manikin statures and vehicle configurations. As it currently works, all manikins in a family follow the same optimisation values without considering different postures for different body dimensions and postural variability, as unlikely happens in reality (Kyung and Nussbaum, 2009; Park et al., 2016b; Brolin et al., 2020; Bubb et al., 2021). Developing a more tailored set of optimal driving angles that consider the unique body dimensions and postural tendencies of different stature groups and for specific types of vehicles could enhance the accuracy of OPM. For example, developing separate sets of optimal angles for distinct manikin sizes or vehicle configurations would allow the optimisation process to better reflect the variability in human posture. Such refinements could significantly improve the method's ability to predict driving postures across a diverse population.

While this case study is grounded in automotive design, the trade-offs between statistical and optimisation-based methods may also be relevant in other DHM application domains such as aerospace or industrial workstation design, where ergonomic requirements vary widely across configurations.

5 Conclusions

This case study provides a comparative evaluation of two posture prediction methods, a statistical regression-based method (SPM) and a specific implementation of an optimisation-based method (OPM) within the DHM tool IPS IMMA. The outcomes from the two methods are compared with real-world data from two vehicles with contrasting seat configurations. While both methods demonstrated potential in predicting seated postures, their performance varied depending on the specific vehicle and prediction point analysed. In this context, SPM, which uses closed-form equations, showed better alignment with measured data for Vehicle B, particularly in predicting vertical H-point positioning. In contrast, OPM, which uses an optimisation approach based on human body models and optimal joint angles, performed better for Vehicle A in fore-aft positioning, possibly due to the default optimal angles being more suited to low-seat configurations. These findings are specific to the implementations and vehicle setups used in this study and should not be generalised to all SPM or OPM methods. Nonetheless, they provide valuable insight for designers working with similar configurations. For example, the Bland-Altman analysis revealed that SPM, in some cases, has a narrower LOA, reflecting greater precision despite the systematic bias. OPM has the ability to incorporate a broader range of ergonomic factors, such as joint angles and constraints, providing a comprehensive and flexible approach for occupant packaging design. However, further refinement is required to improve its performance for diverse and specific populations and vehicle configurations.

In conclusion, this case study illustrates that both driver posture prediction methods have their strengths and weaknesses, and the specific design context, the vehicle configuration, and the need for precision in certain prediction points should guide the choice between them. SPM is considered ideal for quick predictions and situations where computational simplicity is required, while OPM is considered better suited for more complex occupant packaging designs. Furthermore, these methods should not be limited to drivers but also be extended to the design of seating positions for other occupants in the vehicle, such as passengers. Considering the varying needs and postures of different vehicle occupants is crucial for optimising comfort and ergonomics across all seating positions. These results provide human factors practitioners and DHM users with actionable insights into when and how to apply each method depending on design constraints and occupant diversity. This is particularly important as occupant posture prediction becomes more complex in emerging contexts such as autonomous vehicles, where non-driving activities and varied seating configurations are expected. Future research should therefore explore how both SPM and OPM can be adapted to support the design of flexible and comfortable interior layouts that accommodate a broader range of occupant behaviours and needs.

Integrating these methods into the early stages of vehicle occupant packaging design can enhance the overall comfort and safety of vehicle interiors by ensuring that diverse driver populations are better accommodated. Future research should focus on refining both methods, particularly enhancing OPM's adaptability to broader vehicle types, body sizes, and occupant roles (e.g., passengers) and activities (e.g., non-driving tasks), and improving SPM's ability to handle more varied constraints could extend its utility. Further comparative evaluations across a broader range of vehicle types and DHM tool implementations would help establish more generalisable findings and support more informed design decisions in occupant packaging.

Acknowledgements

This work has been made possible with support from the Knowledge Foundation in Sweden (KKS) in the ADOPTIVE project, and SAFER – Vehicle and Traffic Safety Centre at Chalmers, Sweden, and by the participating organisations. This support is gratefully acknowledged.

Declarations

All authors declare that they have no conflicts of interest.

The data used in this study was collected internally by Volvo Cars as part of their established evaluation procedures for occupant packaging design. All participants were company employees who participated voluntarily, in accordance with the company's internal protocols. No personally identifiable information was shared with the researchers, and all data was fully anonymised before analysis. The researchers were granted access to the anonymised dataset for the purpose of academic research and publication.

References

Bergman, C., Castro, P.R., Högberg, D. and Hanson, L. (2015) 'Implementation of suitable comfort model for posture and motion prediction in DHM supported vehicle design', *Procedia Manufacturing*, Vol. 3, pp.3753–3758, https://doi.org/10.1016/j.promfg.2015.07.816.

Bohlin, R., Delfs, N., Hanson, L., Högberg, D. and Carlson, J. (2012) 'Automatic creation of virtual manikin motions maximizing comfort in manual assembly processes', Jack Hu, S. (Eds.): *Proceedings of the 4th CIRP Conference on Assembly Technologies and Systems. Conference on Assembly Technologies and Systems* (*CIRP*), University of Michigan, Ann Arbor, USA.

Brolin, E. (2025) 'Virtual-Driver-Lua: Lua scripts to perform driver ergonomics simulations and evaluations in the IPS software', *GitHub Repository*, https://doi.org/10.5281/zenodo.17073325.

Brolin, E., Högberg, D. and Nurbo, P. (2020) 'Statistical posture prediction of vehicle occupants in digital human modelling tools', Duffy, V. (Ed.): *Digital Human Modeling and Applications in Health, Safety, Ergonomics and Risk Management. Posture, Motion and Health*, Lecture Notes in Computer Science, Vol. 12198, https://doi.org/10.1007/978-3-030-49904-4_1.

Bubb, H., Bengler, K., Grünen, R.E. and Vollrath, M. (2021) *Automotive Ergonomics*, Springer Fachmedien Wiesbaden, https://doi.org/10.1007/978-3-658-33941-8.

Delfs, N., Bohlin, R., Hanson, L., Högberg, D. and Carlson, J. (2013) 'Introducing stability of forces to the automatic creation of digital human postures', *Second International Digital Human Modeling Symposium*, DHM 2013, Ann Arbor, USA.

Demirel, H.O., Ahmed, S. and Duffy, V.G. (2021) 'Digital human modeling: a review and reappraisal of origins, present, and expected future methods for representing humans computationally', *International Journal of Human–Computer Interaction*, pp.1–41, https://doi.org/10.1080/10447318.2021.1976507.

Hanson, L., Högberg, D., Carlson, J.S., Delfs, N., Brolin, E., Mårdberg, P., Spensieri, D., Björkenstam, S., Nyström, J. and Ore, F. (2019) 'Chapter 11 – industrial path solutions – intelligently moving manikins', in Scataglini, S. and Paul, G. (Eds.): *DHM and Posturography*, pp.115–124, Academic Press, https://doi.org/10.1016/B978-0-12-816713-7.00011-8.

Hanson, L., Sperling, L. and Akselsson, R. (2006) 'Preferred car driving posture using 3-D information', *International Journal of Vehicle Design*, Vol. 42, Nos. 1–2, p.154, https://doi.org/10.1504/IJVD.2006.010183.

Huston, F.J., Zielinski, G.L., Reed, M.P., Huston, F.J., Zielinski, G.L. and Reed, M.P. (2024) 'Creation of the driver fixed heel point (Fhp) CAD accommodation model for military ground vehicle design', *SAE Technical Paper* 2024-01-3582, November 15, https://doi.org/10.4271/2024-01-3582.

IPS IMMA (2025) [online] https://industrialpathsolutions.se/ips-imma (accessed 9 September 2025).

Jeong, Y., Lee, G., Beck, D. and Park, W. (2023) 'Effects of driver personal variables on preferred vehicle interior components setting', *International Journal of Industrial Engineering: Theory, Applications and Practice*, Vol. 30, No. 1, p.1, https://doi.org/10.23055/ijietap.2023.30.1.8495.

Jonsson, B., Stenlund, H., Svensson, M.Y. and Björnstig, U. (2008) 'Seat adjustment – capacity and repeatability among occupants in a modern car', *Ergonomics*, Vol. 51, No. 2, pp.232–241, https://doi.org/10.1080/00140130701561793.

Jung, J. and Park, W. (2023) 'An exploratory study on the characteristics of drivers' preferred seat positions', *International Journal of Industrial Engineering: Theory, Applications and Practice*, Vol. 30, No. 4, p.4, https://doi.org/10.23055/ijietap.2023.30.4.8723.

Kyung, G. and Nussbaum, M.A. (2009) 'Specifying comfortable driving postures for ergonomic design and evaluation of the driver workspace using digital human models', *Ergonomics*, Vol. 52, No. 8, pp.939–953, https://doi.org/10.1080/00140130902763552.

Lejon, N. and Thorsén, H. (2013) *Exploring Drivers' Seated Position – Method Development Within Automotive Ergonomics*, MSc Thesis, Chalmers University of Technology, Sweden [online] https://hdl.handle.net/20.500.12380/178438 (accessed 19 February 2025).

Parida, S., Abanteriba, S. and Franz, M. (2020) 'Digital human modelling, occupant packaging and autonomous vehicle interior', in Ahram, T., Karwowski, W., Pickl, S. and Taiar, R. (Eds.): *Human Systems Engineering and Design II*, pp.202–208, Springer International Publishing, https://doi.org/10.1007/978-3-030-27928-8_31.

Park, J., Ebert, S.M., Reed, M.P. and Hallman, J.J. (2016a) 'A statistical model including age to predict passenger postures in the rear seats of automobiles', *Ergonomics*, Vol. 59, No. 6, pp.796–805, https://doi.org/10.1080/00140139.2015.1088076.

Park, J., Ebert, S.M., Reed, M.P. and Hallman, J.J. (2016b) 'Statistical models for predicting automobile driving postures for men and women including effects of age. human factors', *The Journal of the Human Factors and Ergonomics Society*, Vol. 58, No. 2, pp.261–278, https://doi.org/10.1177/0018720815610249.

Park, S.J., Min, S., Subramaniyam, M., Lee, H., Shin, Y., Jang, C. and Hwang, S. (2015) 'Driving posture measurement using 3d scanning measuring technique', *SAE International Journal of Passenger Cars – Mechanical Systems*, Vol. 8, https://doi.org/10.4271/2015-01-1392.

Parkinson, M.B. and Reed, M.P. (2006) *Optimizing Vehicle Occupant Packaging, in: Reliability and Robust Design in Automotive Engineering 2006* (SP-2032), SAE Technical Paper Series. Presented at the SAE 2006 World Congress and Exhibition, SAE Global Mobility Database, Detroit, Michigan, pp.2006-01–0961, https://doi.org/10.4271/2006-01-0961.

Peng, J., Wang, X., and Denninger, L. (2018) 'Effects of anthropometric variables and seat height on automobile drivers' preferred posture with the presence of the clutch', *Human Factors: The Journal of the Human Factors and Ergonomics Society*, Vol. 60, No. 2, pp.172–190, https://doi.org/10.1177/0018720817741040.

Perez Luque, E., Brolin, E., Lamb, M. and Högberg, D. (2022) 'Simulation of hip joint location for occupant packaging design', *Proceedings of the 7th International Digital Human Modeling Symposium* (*DHM 2022*) *and Iowa Virtual Human Summit 2022*, Vol. 7, No. 1, p.1, https://doi.org/10.17077/dhm.31742.

Porter, J.M. and Gyi, D. (1998) 'Exploring the optimum posture for driver comfort', *International Journal of Vehicle Design*, Vol. 29, pp.255–266, https://doi.org/10.1504/IJVD.1998.062075.

Raschke, U. and Cort, C. (2019) 'Chapter 3 – Siemens Jack', in Scataglini, S. and Paul, G. (Eds.): *DHM and Posturography*, pp.35–48, Academic Press, https://doi.org/10.1016/B978-0-12-816713-7.00003-9.

Reed, M.P. (2013) 'Driver preference for fore-aft steering wheel location', *SAE International Journal of Passenger Cars – Mechanical Systems*, Vol. 6, No. 2, pp.629–635, https://doi.org/10.4271/2013-01-0453.

Reed, M.P., Manary, M.A., Flannagan, C.A.C. and Schneider, L.W. (2000) *Comparison of Methods for Predicting Automobile Driver Posture*, SAE Technical Paper, 2000-01–2180. https://doi.org/10.4271/2000-01-2180

Reed, M.P., Manary, M.A., Flannagan, C.A.C. and Schneider, L.W. (2002) 'A statistical method for predicting automobile driving posture', *Human Factors: The Journal of the Human Factors and Ergonomics Society*, Vol. 44, No. 4, pp.557–568, https://doi.org/10.1518/0018720024496917.

SAE J1100 (2009) *J1100_200911: Motor Vehicle Dimensions – SAE International* [online] https://www.sae.org/standards/content/j1100_200911 (accessed 19 February 2025).

SAE J3099 (2024) *J3099_202405: Driver Seating Accommodation and Steering Wheel Location Models – SAE International* [online] https://www.sae.org/standards/content/j3099_202405 (accessed 19 February 2025).

SAE J941 (2010) *J941_201003: Motor Vehicle Drivers' Eye Locations – SAE International* [online] https://www.sae.org/standards/content/j941_201003 (accessed 19 February 2025).

Scataglini, S. and Paul, G. (2019) *DHM and Posturography*, Academic Press, Elsevier.

Schmidt, S., Amereller, M., Franz, M., Kaiser, R. and Schwirtz, A. (2014) 'A literature review on optimum and preferred joint angles in automotive sitting posture', *Applied Ergonomics*, Vol. 45, No. 2, pp.247–260, https://doi.org/10.1016/j.apergo.2013.04.009.

Seidl, A. (1994) *Das Menschmodell RAMSIS: Analyse, Synthese und Simulation dreidimensionaler Körperhaltungen des Menschen*, Doctoral Dissertation, Technical University of Munich, Germany.

Society of Automotive Engineers (SAE) J1100 (2009) *Motor Vehicle Dimensions*, Society of Automotive Engineers, Inc., Warrendale, PA [online] https://www.sae.org/standards/content/j1100_200911 (accessed 19 February 2025).

Wirsching, H-J. (2019) 'Chapter 4 – human solutions RAMSIS', in Scataglini, S. and Paul, G. (Eds.): *DHM and Posturography*, pp.49–55), Academic Press, https://doi.org/10.1016/B978-0-12-816713-7.00004-0.

Wolf, A., Miehling, J. and Wartzack, S. (2020) 'Challenges in interaction modelling with digital human models – a systematic literature review of interaction modelling approaches', *Ergonomics*, Vol. 63, No. 11, pp.1442–1458, https://doi.org/10.1080/00140139.2020.1786606.

Wolf, P., Hennes, N., Rausch, J. and Potthast, W. (2022) 'The effects of stature, age, gender, and posture preferences on preferred joint angles after real driving', *Applied Ergonomics*, Vol. 100, p.103671, https://doi.org/10.1016/j.apergo.2021.103671.

Wu, J., Liu, J., Li, X., Yan, L., Cao, L. and Zhang, H. (2022) 'Recognition and prediction of driver's whole body posture model', *Proceedings of the Institution of Mechanical Engineers, Part D: Journal of Automobile Engineering*, Vol. 236, No. 14, pp.3326–3343, https://doi.org/10.1177/09544070211068676.

Yang, J., Marler, T., Kim, H., Farrell, K., Mathai, A., Beck, S., Abdel-Malek, K., Arora, J. and Nebel, K. (2005) *SantosTM: A New Generation of Virtual Humans*, SAE Technical Paper, 2005-01–1407, https://doi.org/10.4271/2005-01-1407.

Appendix

This appendix presents Bland-Altman plots for comparing predicted and measured values across key prediction points for SPM and OPM. These plots provide a visual representation of the methods' precision and adaptability, highlighting the differences between predictions and real-world data in the specific design contexts examined in this case study. In each plot, the solid horizontal line represents the mean bias, which is the average difference between the predicted and measured values, indicating whether a method tends to systematically overpredict or underpredict. The dashed horizontal lines represent the limits of agreement (LOA), showing the range within which most differences are expected to fall. Narrow LOA indicate higher precision, while the distribution and pattern of the data points offer insights into each method's adaptability and systematic behaviour.

Figure A1 Bland-Altman plots comparing H-point x predictions for (a) SPM and (b) OPM in (c) Vehicle A and (d) Vehicle B (see online version for colours)

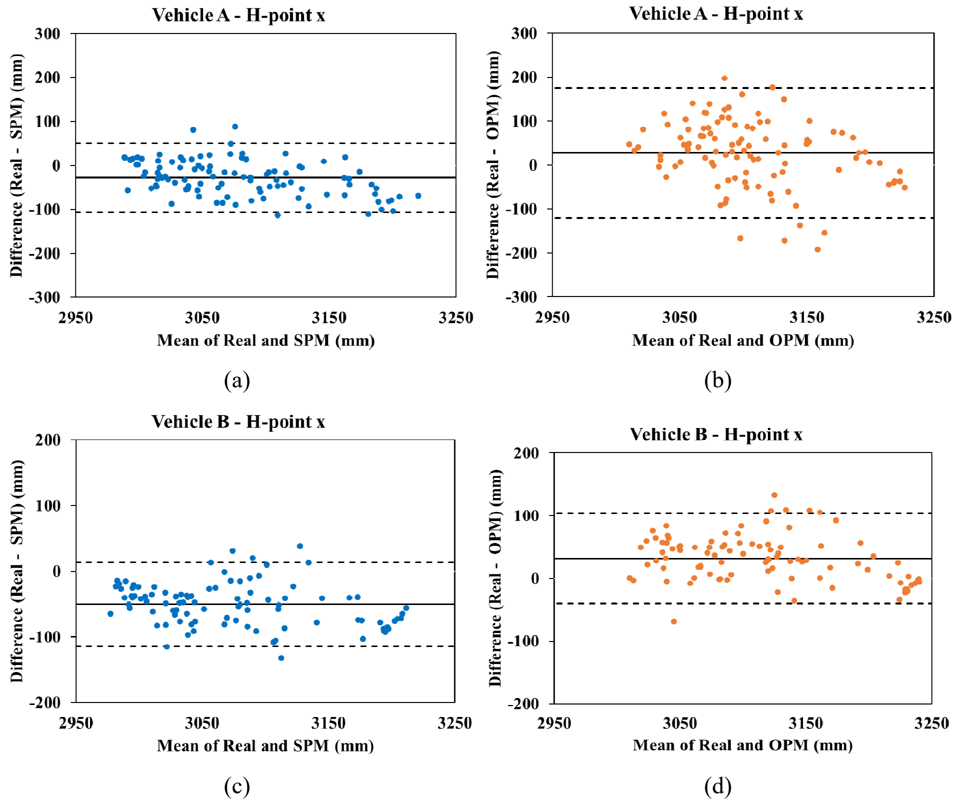

Figure A2 Bland-Altman plots comparing H-point z predictions for (a) SPM and (b) OPM in (c) Vehicle A and (d) Vehicle B (see online version for colours)

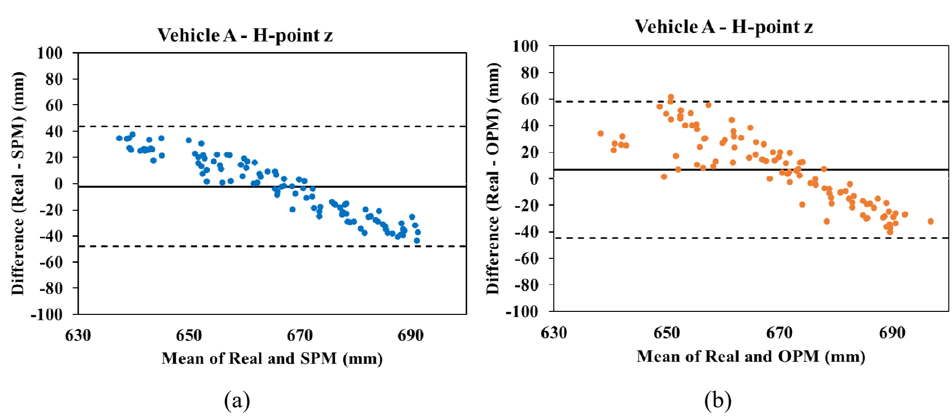

Figure A2 Bland-Altman plots comparing H-point z predictions for (a) SPM and (b) OPM in (c) Vehicle A and (d) Vehicle B (continued) (see online version for colours)

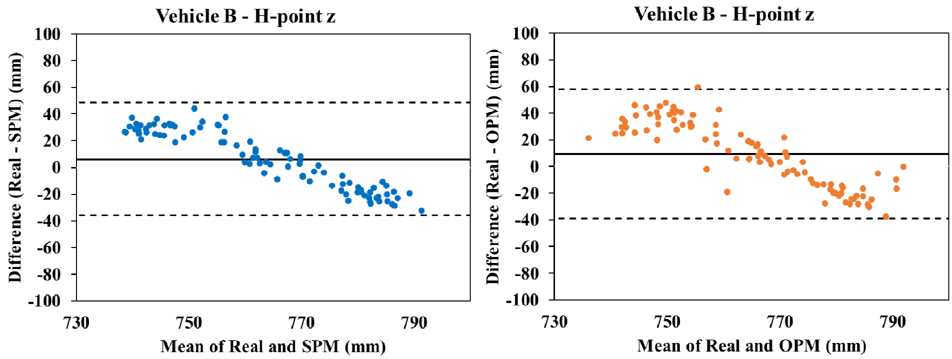

(c) (d)

Figure A3 Bland-Altman plots comparing eye-point x predictions for (a) SPM and (b) OPM in (c) Vehicle A and (d) Vehicle B (see online version for colours)

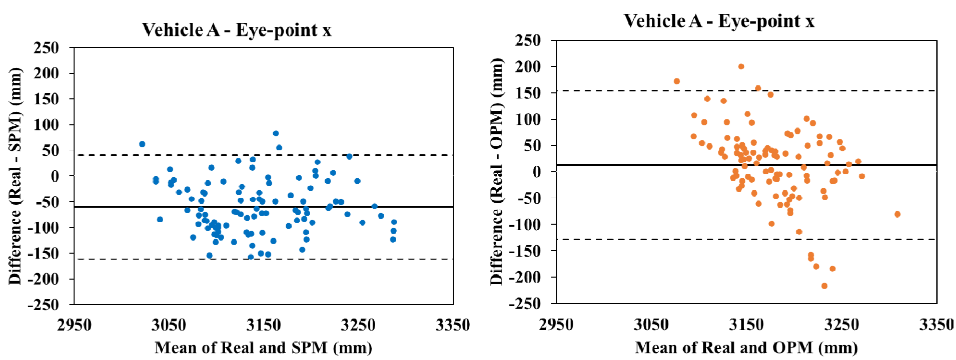

(a) (b)

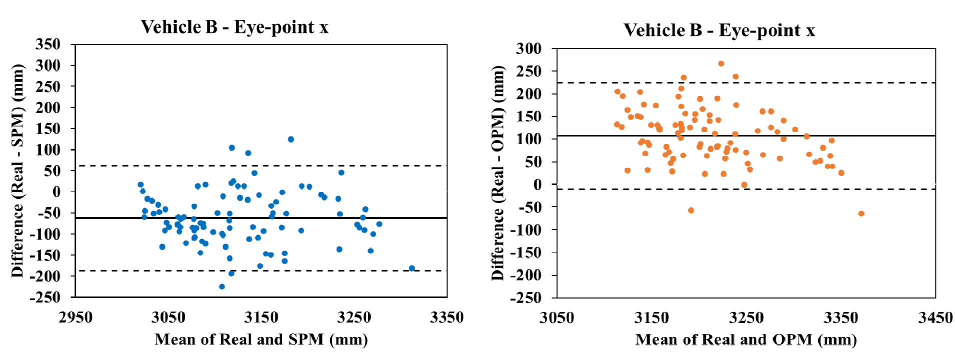

(c) (d)

Figure A4 Bland-Altman plots comparing Eye-point x predictions for (a) SPM and (b) OPM in (c) Vehicle A and (d) Vehicle B (see online version for colours)

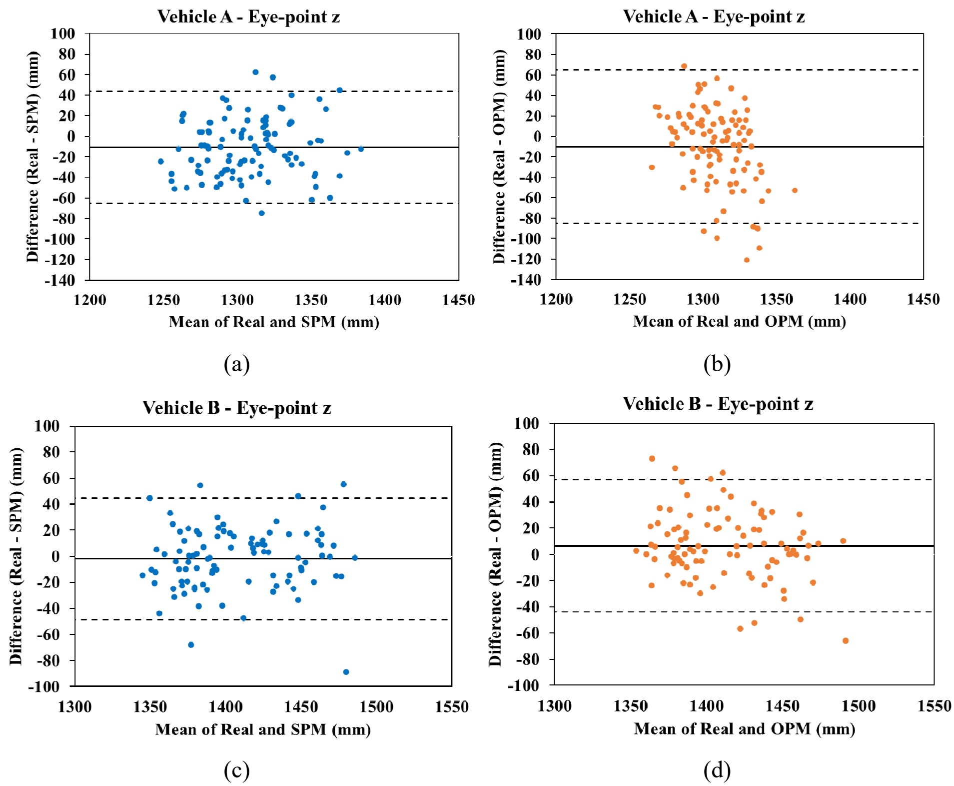

Figure B1 Euclidean distances between predicted and observed values for SPM and OPM across H-point (a) and Eye-point (b) positions in (c) Vehicle A and (d) Vehicle B (see online version for colours)

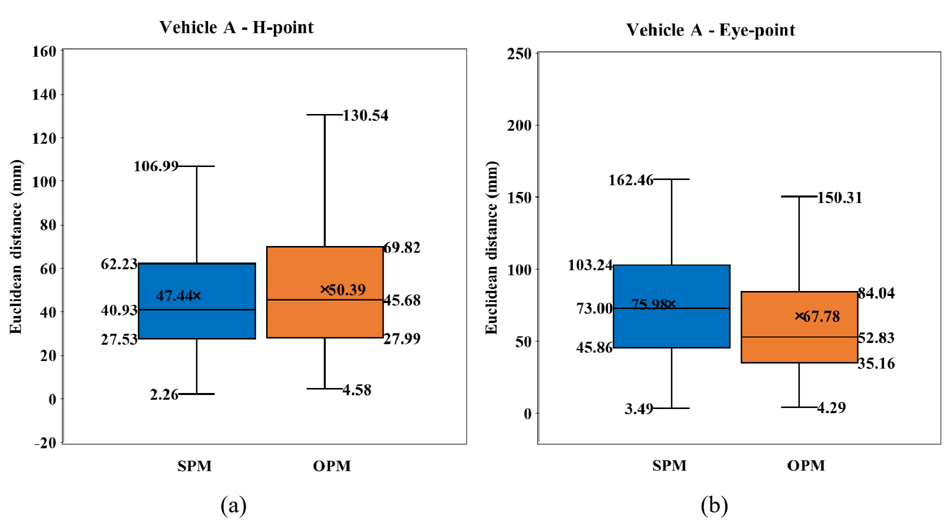

Figure B1 Euclidean distances between predicted and observed values for SPM and OPM across H-point (a) and Eye-point (b) positions in (c) Vehicle A and (d) Vehicle B (continued) (see online version for colours)

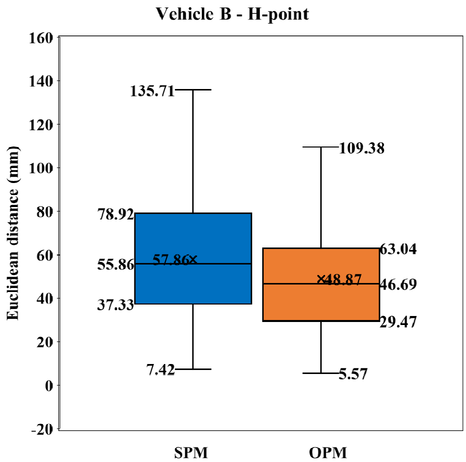

(c)

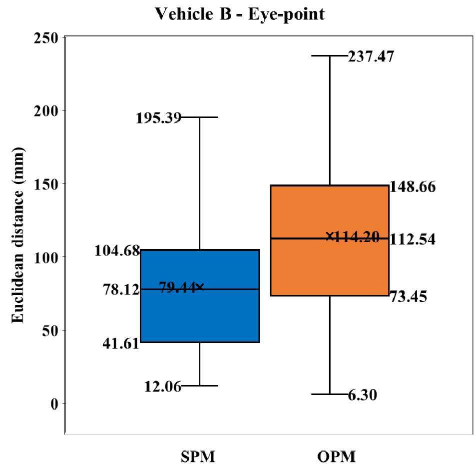

(d)